SAND2017-10522C

Nonlinear Power Flow Control Design for Networked AC/DC Based Microgrid Systems

David G. Wilson
Electrical Science & Experiments Department, Sandia National Laboratories, P.O. Box 5800, Albuquerque, NM 87185-1152, dwilso@sandia.gov
Wayne W. Weaver
Electrical and Computer Engineering, 121 EERC Building, 1400 Townsend Drive, Michigan Technological University, Houghton, MI 49931-1295, wwweaver@mtu.edu
Rush D. Robinett, III
Mechanical Engineering-Engineering Mechanics, R.L. Smith Bldg 903, 1400 Townsend Drive, Michigan Technological University, Houghton, MI 49931, rdrobine@mtu.edu
Steve F. Glover
Electrical Science & Experiments Department, Sandia National Laboratories, P.O. Box 5800, Albuquerque, NM 87185-1152, sfglove@sandia.gov

***Abstract*— This paper presents a control design methodology that addresses high penetration of variable generation or renewable energy sources and loads for networked AC/DC microgrid systems as an islanded subsystem or as part of larger electric power grid systems. High performance microgrid systems that contain large amounts of stochastic sources and loads is a major goal for the future of electric power systems. Alternatively, methods for controlling and analyzing AC/DC microgrid systems will provide an understanding into the tradeoffs that can be made during the design phase. This method develops both a control design methodology and realizable hierarchical controllers that are based on the Hamiltonian Surface Shaping and Power Flow Control (HSSPFC) [1] methodology that regulates renewable energy sources, varying loads and identifies energy storage requirements for a networked AC/DC microgrid system. Both static and dynamic stability conditions are derived. A renewable energy scenario is considered for a networked three DC microgrids tied into an AC ringbus configuration. Numerical simulation results are presented.**

Keywords - *decentralized control; microgrid; nonlinear control; energy storage; stochastic sources*

I. Introduction

Recent literature has indicated that there exists a trade-off in information and power flow and that intelligent, coordinated control of power flow in a microgrid system can modify energy storage hardware requirements. In [2] a new decentralized robust strategy was proposed to improve small and large-signal stability, power sharing of hybrid AC/DC microgrids, and improve the performance for nonlinear and unbalanced loads. The future electric power grid and corresponding microgrid systems will require new mathematical tools and methodologies to support high penetration of renewable energy sources such as solar and wind and provide specific optimized designs. Current unidirectional power flow from source to load will be replaced by bi-directional power flow as new generation sources are being distributed onto the future electric power grid. Renewable and other distributed energy sources cannot be economically and reliably integrated into the existing grid because it has been optimized over decades to support large centralized generation sources. The review in [3] was focused on hierarchical controls which covers three main levels. The researchers identified that future control trends needed further research in interconnected microgrids. Reference [4] summarized the problems and solutions of power quality in microgrids, distributed-energy storage systems, and hybrid AC/DC microgrids. Power quality enhancement, cooperative control for voltage enhancement, harmonics, and unbalances in microgrids are reviewed. A static synchronous compensator (STATCOM) in grid-connected microgrid was introduced to improve voltage sags/swells and unbalance. In [5] a model was developed to study the impact of power sharing controllers and delays in microgrid stability. The effectiveness of the proposed controller was presented through comparative simulation and experimental results. In [6] advanced control techniques are reviewed. The review covers decentralized, distributed, and hierarchical control of grid-connected and islanded microgrids. Recent developments included stability anaysis of decentralized controlled microgrids.

Today's grid model is based on excess generation capacity (largely fossil fuel), static distribution/transmission systems, and essentially open loop control of power flow between sources and loads. Research investments in future grid modernization and microgrids are presently being made by the Department of Energy, Department of Defense, and others [2], [3], [4], [5], [6], [7], [8], [9]. Other approaches have been developed that optimize distributed energy systems to improve efficiency of the energy resources [10].

Achieving regulation and power balance in a system with high penetration levels of stochastic renewable sources are some of the challenges addressed by this research. The problem is solved provided *enough* energy storage is available. Realistically, energy storage systems and/or information flow are costly and both need to be minimized and balanced with respect to the performance objectives.

Distribution of energy storage and power conversion in the microgrid can be achieved by providing an architecture with three parts: the feedforward or dynamic optimization control, the Hamiltonian-based feedback control, and the servo control. A centralized algorithm provides feedforward control by computing reference duty cycle values and reference states at a much slower update rate that optimizes a cost function that may include boost converter set point update rates, energy storage use, and/or parasitic losses in the system. The feedforward control identifies the optimal operating point and can be determined using Sequential Quadratic Programming (SQP) or dynamic programming methods [11], [12], [13]. For this investigation a very simple steady state solution is realized as a proof-of-concept. The Hamiltonian-based control is a local decentralized feedback controller that is designed to minimize variability in the power delivered to the boost converters [1], [7], [9], [12], [14], [15]. The servo control supports the Hamiltonian-based control by regulating certain components to specified voltages at the fastest update rates which corresponds to the actual boost converter hardware inputs.

This paper is discussed in five sections. In Section II an AC/DC reduced order networked microgrid model is presented. In Section III, the HSSPFC controller design for the AC/DC networked microgrid is developed which includes both the feedforward and feedback developments. In Section IV numerical simulations are performed that validate and demonstrate proof-of-concept for the proposed HSSPFC designs, and finally in Section V the results are summarized.

II. Reduced Order AC/DC Networked Microgrid Model

The goal of Reduced Order Models (ROMs) are to capture the critical dynamics of the microgrid system for control system design and refererence model trajectories as part of the feedforward system with correction being applied by the feedback system. ROMs were initially developed as part of the HSSPFC design process [1] during a microgrid control project [21] project. Models were developed for separate single/networked DC microgrid systems[12], [17], [7], [19], [9] and AC microgrid systems [16], [18]. The initial model for an AC/DC system for a single inverter was developed in [16] and employed for HSSPFC control design in [18]. In the next subsection this model is briefly discussed and the full details leading into the novel networked AC/DC microgrids and HSSPFC control are developed further.

A. Single AC/DC Microgrid

The AC inverter microgrid model is based on a single boost converter (full details for this model are given in [16], [18]). It is fed by voltage sources, representing variable/stochastic renewable energy sources such as wind or solar, in series with an energy storage source. These are connected to a DC bus that is then connected to a 3-phase AC bus through the inverter. The 3-phase AC system and load is modeled through DQ reference frame transformation as an equivalent 2-phase DC network. An energy storage source is also connected to the AC bus to inject power onto the AC bus to support variations in the load. The AC microgrid system is shown in Fig. 1.

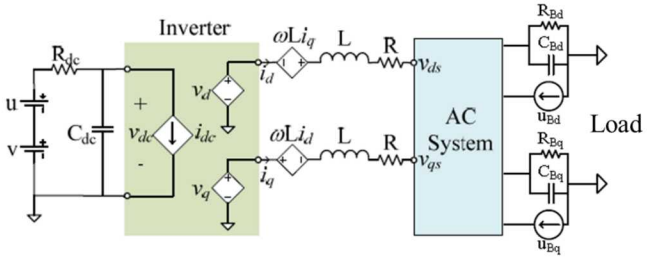

Fig. 1. AC inverter model with energy storage controls at input and load characterized as part of the 0DQ decomposition.

The circuit equations for the DC-AC converter and AC bus models are given in [16]. The transformed three-phase inverter in 0DQ frame is defined as

$$\begin{array}{rcl} L\frac{di_d}{dt} & = & -Ri_d + \omega L i_q + v_d - v_{d_s} \\ L\frac{di_q}{dt} & = & -Ri_q - \omega L i_d + v_q - v_{q_s} \end{array} \tag{1}$$

with

$$v_{d_q} = \left\{ \begin{array}{c} 0 \\ v_d \\ v_q \end{array} \right\} = \left\{ \begin{array}{c} 0 \\ \beta\lambda c\phi \\ \beta\lambda s\phi \end{array} \right\} v_{dc} \tag{2}$$

where $\beta = \frac{1}{2}\sqrt{\frac{3}{2}}$, $c\phi = \cos\phi$, and $s\phi = \sin\phi$. Simplifying the equations yields

$$\begin{array}{rcl} L\frac{di_d}{dt} & = & -Ri_d + \omega L i_q + \beta\lambda c\phi - v_{d_s} \\ L\frac{di_q}{dt} & = & -Ri_q - \omega L i_d + \beta\lambda s\phi - v_{q_s} \\ C_{dc}\frac{dv_{dc}}{dt} & = & (v_1 + u_1 - v_{dc})/R_{dc} - \beta\lambda(c\phi i_d + s\phi i_q). \end{array} \tag{3}$$

The AC bus equations become [16]

$$\begin{array}{rcl} C_B\frac{dv_{ds}}{dt} & = & i_d - \frac{v_{d_s}}{R_B} + u_{B_d} + \omega C_B v_{qs} \\ C_B\frac{dv_{qs}}{dt} & = & i_q - \frac{v_{q_s}}{R_B} + u_{B_q} - \omega C_B v_{ds}. \end{array} \tag{4}$$

This development serves as a basis for the networked AC/DC microgrid model development given next. Details for a single AC/DC microgrid system and HSSPFC controller can be found in [18].

B. Networked AC/DC microgrid

The networked AC/DC microgrid ROM is develped based on the following assumptions; i) the diesel engine dynamics are simplified and replaced by a DC

source, storage device, and boost converter. The standard engine-to-DC generator is given in Fig. 2, where the engine is the prime mover and source of rotational energy. The synchronous machine converts rotational speed to AC voltage (torque to AC current) and the rotating mass is inertial stored energy and can be converted to AC voltage. The passive rectifier converts AC to unregulated DC voltage. The DC/DC converter provides active conversion to a regulated DC bus. The reduced order DC source model assumptions include; a) the engine and machine fast dynamics are ignored, b) the engine slow dynamics are caputred by $v_{s,k}$ (source), c) the spinning inertia energy dynamics are captured by $u_{s,k}$ (storage), d) the impedance dynamics are lumped into the DC line, and e) the DC/DC converter ignores the switching dynamics and uses only the average mode (slow dynamics). The simplified model is represented as the circuit diagram at the far left in Figs. 3 and 4, respectively. ii) The battery and DC/DC converter are

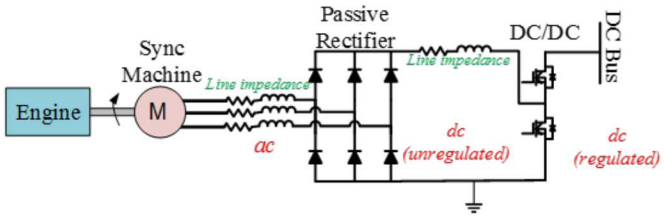

Fig. 2. Standard engine-to-DC generator schematic.

modeled as a DC current injection storage device. iii) The DC/AC inverter is modeled as a loss-less power balance between DC and DQ. A standard DC/AC model employs six switches (FET or IGBT) to convert DC voltageg to regulated three-phase AC. Switching PWM signals generate three-phase voltage output [16]. The reduced order inverter model assumptions include; a) the switching is fast and lossless (negligible) and the DC power equals the AC power which uses dependent sources to balance power. b) the three-phase AC has a synchronous reference frame (see [16]). This includes; a) the frequency is fixed, b) a-b-c phases can be directly converted to two-phase (DC like) DQ reference frame and b) three-phase line impedance can be directly converted into DQ model (including current dependent voltage sources). Finally, iv) the lines of the AC ring-bus are sufficiently short to ignore line dynamics and models the ring as a single AC bus.

The fundamental DC microgrid model (see Fig. 1) is generalized from the previous section by introducing a single DC microgrid module k as shown in Fig. 3. This fundamental building block can be used to build a large number of DC microgrid systems ($k = 1, \ldots, N$) that tie into an AC ring bus. For this development we will be investigating three DC microgrids ($k = 3$) that tie into an AC ring bus. It can also serve to represent a single AC/DC microgrid ROM system.

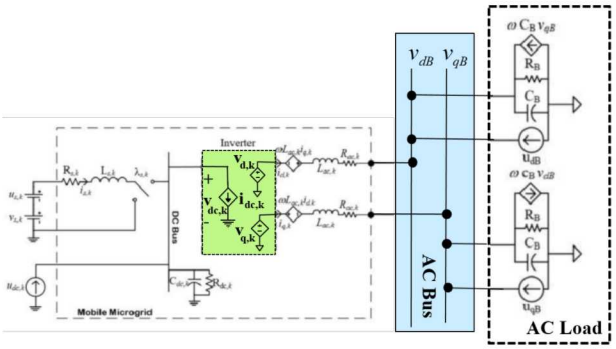

Fig. 3. Single microgrid module k.

The detailed schematic for the networked microgrid dynamics is shown in Fig. 4.

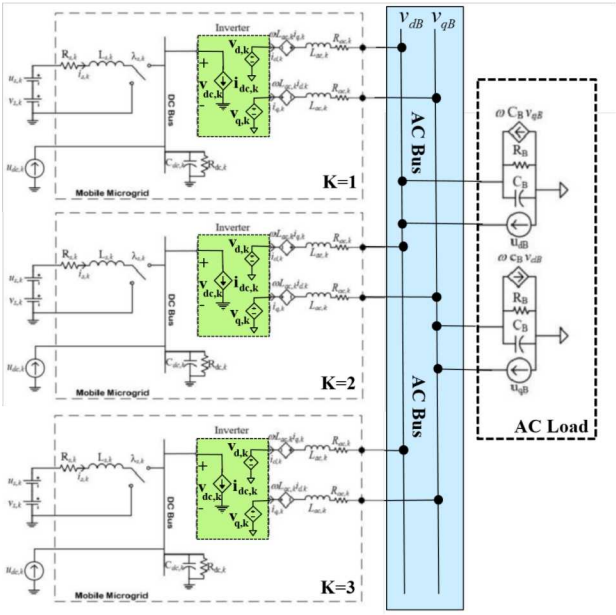

Fig. 4. Networked microgrid system.

The system model for the microgrid DC and AC converters is

$$\begin{aligned} L_{s,k}\frac{di_{s,k}}{dt} &= -\lambda_{s,k}v_{dc,k} - R_{s,k}i_{s,k} + u_{s,k} + v_{s,k} \\ C_{dc,k}\frac{dv_{dc,k}}{dt} &= -i_{dc,k} - \frac{v_{dc,k}}{R_{dc,k}} + u_{dc,k} + \lambda_{s,k}i_{s,k} \\ L_{ac,k}\frac{di_{d,k}}{dt} &= -R_{ac,k}i_{d,k} + \omega L_{ac,k}i_{q,k} + v_{d,k} - v_{dB} \\ L_{ac,k}\frac{di_{q,k}}{dt} &= -\omega L_{ac,k}i_{d,k} - R_{ac,k}i_{q,k} + v_{q,k} - v_{qB} \end{aligned} \tag{5}$$

where $u_{s,k}$ is a model of a storge device on the AC generator connection and $u_{dc,k}$ is the equivalent current injection from the battery storage device.

The inverter model control is given as

$$\begin{aligned} v_{d,k} &= = \beta\lambda_{dc,k}v_{dc,k}c(\phi_{dc,k}) \\ v_{d,k} &= = \beta\lambda_{dc,k}v_{dc,k}s(\phi_{dc,k}) \end{aligned} \tag{6}$$

where $\lambda_{dc,k}$ is the inverter control variable of the AC voltage magnitude, $\phi_{dc,k}$ is the inverter control variable of the AC voltage phase, $\beta = \frac{1}{2}\sqrt{\frac{3}{2}}$, $c = \cos$, and $s = \sin$.

The DC current into the inverter is

$$i_{dc,k} = \beta\lambda_{dc,k}[c(\phi_{dc,k})i_{d,k} + s(\phi_{dc,k})i_{q,k}] \quad (7)$$

Susbtitute the control back into the system model yields

$$L_{s,k}\frac{di_{s,k}}{dt} = -\lambda_{s,k}v_{dc,k} - R_{s,k}i_{s,k} + u_{s,k} + v_{s,k} \quad (8)$$

$$C_{dc,k}\frac{dv_{dc,k}}{dt} = -\beta\lambda_{dc,k}[c(\phi_{dc,k})i_{d,k} + s(\phi_{dc,k})i_{q,k}] - \frac{v_{dc,k}}{R_{dc,k}} + u_{dc,k} + \lambda_{s,k}i_{s,k} \quad (9)$$

$$L_{ac,k}\frac{di_{d,k}}{dt} = -R_{ac,k}i_{d,k} + \omega L_{ac,k}i_{q,k} + \beta\lambda_{dc,k}v_{dc,k}c(\phi_{dc,k}) - v_{dB} \quad (10)$$

$$L_{ac,k}\frac{di_{q,k}}{dt} = -\omega L_{ac,k}i_{d,k} - R_{ac,k}i_{q,k} + \beta\lambda_{dc,k}v_{dc,k}s(\phi_{dc,k}) - v_{qB} \quad (11)$$

along with the AC bus model determined as

$$\begin{array}{rcl} C_B\frac{dv_{dB}}{dt} & = & \sum_d i_{d,k} + \omega C_B v_{qB} - \frac{v_{dB}}{R_B} + u_{dB} \\ C_B\frac{dv_{qB}}{dt} & = & \sum_q i_{q,k} - \omega C_B v_{dB} - \frac{v_{qB}}{R_B} + u_{qB} \end{array} \quad (12)$$

The reduced order model is defined in matrix form as

$$\begin{array}{rcl} \mathbf{M}\dot{\mathbf{x}} & = & \mathbf{R}\mathbf{x} + \mathbf{D}^T\mathbf{v} + \mathbf{B}^T\mathbf{u} \\ & = & [\bar{\mathbf{R}} + \tilde{\mathbf{R}}]\mathbf{x} + \mathbf{D}^T\mathbf{v} + \mathbf{B}^T\mathbf{u} \end{array} \quad (13)$$

where $\mathbf{R} = \bar{\mathbf{R}} + \tilde{\mathbf{R}}$ is composed of a symmetric and skew-symmetric matrices, respectively.

The states, controls, and input vectors are defined as

$$\begin{array}{rcl} \mathbf{x} & = & [i_{sj}\ v_{dcj}\ i_{dj}\ i_{qj}\ v_{dB}\ v_{qB}]^T \\ & & j = 1 \ldots 3 \\ \mathbf{u} & = & [u_{s1}\ u_{s2}\ u_{s3}\ u_{dc1}\ u_{dc2}\ u_{dc3}\ u_{dB}\ u_{qB}]^T \\ \mathbf{v} & = & [v_{s1}\ v_{s2}\ v_{s3}]^T. \end{array} \quad (14)$$

III. HSSPFC Control Design for AC/DC Microgrid System

The goal of the HSSPFC design is to define static and dynamic stability criteria for an AC/DC microgrid system. The controller design consists of both feedforward and feedback portions. For the feedforward or guidance algorithm two possible options can be considered; i) a dynamic optimization formulation can be developed in general to accomodate a large number of generation, loads, busses, and energy storage resources (see reference [18], [11]) or ii) a simple steady-state solution to Eq. (13) can be solved (for a DC microgrid system see [12]). The basis of dynamic optimization is to formulate the problem in terms of an optimal control problem [11]. In general, there are three overall goals: reduce the change in the inverter duty cycles, reduce the reliance on the energy storage devices, and reduce the parasitic losses. The AC inverter circuit and bus equations can be expanded to include larger orders and combinations of each. Thus the goal is to minimize an appropriate objective function (or performance index PI). The remainder of this development will focus on the second option (simplified steady state solution).

A. Feedforward Control Based on Steady-State Solution

The feedforward control is based on a balanced power flow

$$\mathbf{x}_R^T\left[\mathbf{M}\dot{\mathbf{x}}_R - (\bar{\mathbf{R}} + \tilde{\mathbf{R}})\mathbf{x}_R - \mathbf{D}^T\mathbf{v} - \mathbf{B}^T\mathbf{u}_R\right] = 0 \quad (15)$$

for which the reference state becomes

$$\mathbf{M}\dot{\mathbf{x}}_R = (\bar{\mathbf{R}} + \tilde{\mathbf{R}})\mathbf{x}_R + \mathbf{D}^T\mathbf{v} + \mathbf{B}^T\mathbf{u}_R. \quad (16)$$

Note the skew-symmetric condition $\mathbf{x}_R^T\tilde{\mathbf{R}}\mathbf{x}_R = 0$. For steady-state operation and generating set points the following equation can be solved for reference states $\mathbf{x_R}$, duty cycles λ, angles ϕ, and with a specified frequency ω as

$$\mathbf{0} = \mathbf{R}\mathbf{x}_R + \mathbf{D}^T\mathbf{v} + \mathbf{B}^T\mathbf{u}_R. \quad (17)$$

An illustrative methodology for a single AC ring bus, the following assumptions are made; i) reference states $x_{13_R} = v_{dB}$ and $x_{14_R} = v_{qB}$ are specified and for balanced power flow the control $\mathbf{u_R} = \mathbf{0}$.

The first step is to determine the necessary network currents as

$$\begin{array}{rcl} I_{d_{total}} & = & \sum_{k=1}^N i_{d,k} = \left[\frac{v_{dB}}{R_B} - \omega C_B v_{qB}\right] \\ I_{q_{total}} & = & \sum_{k=1}^N i_{q,k} = \left[\frac{v_{qB}}{R_B} + \omega C_B v_{dB}\right]. \end{array} \quad (18)$$

By introducing the power proportionment term α_k then

$$\begin{array}{rcl} i_{d,k} & = & \alpha_k I_{d_{total}} \quad \forall \quad k = 1,2,3 \\ i_{q,k} & = & \alpha_k I_{q_{total}} \quad \forall \quad k = 1,2,3 \end{array} \quad (19)$$

where $\sum_k \alpha = 1$.

In step two, the phase angles $\phi_{dc,k}$ are determined for each microgrid k as

$$\begin{array}{rcl} tan\phi_{dc,k} & = & \frac{\omega L_{AC,k}i_{d,k} + R_{AC,k}i_{q,k} + v_{qB}}{R_{AC,k}i_{d,k} - \omega L_{AC,k}i_{q,k} + v_{dB}} \\ y_{dc,k} & = & \omega L_{AC,k}i_{d,k} + R_{AC,k}i_{q,k} + v_{qB} \\ x_{dc,k} & = & R_{AC,k}i_{d,k} - \omega L_{AC,k}i_{q,k} + v_{dB} \\ \phi_{dc,k} & = & TAN2(y_{dc,k}, x_{dc,k}). \end{array} \quad (20)$$

In final step three, the steady state algebraic nonlinear equation $F(x)$ is solved for each individual microgrid k. $F(x)$ contains four states given as

$$x = [\lambda_{s,k}\ \ \lambda_{dc,k}\ \ i_{s,k}\ \ v_{dc,k}]^T = [x_1\ \ x_2\ \ x_3\ \ x_4]^T \quad (21)$$

and the nonlinear equations coupled in the states are given as

$$\begin{array}{l} F_1(x) = -x_1x_4 - R_{s,k}x_3 + v_{s,k} \\ F_2(x) = -\beta(c\phi_{dc,k}i_{d,k} + s\phi_{dc,k}i_{q,k})x_2 - \frac{1}{R_{dc,k}}x_4 + x_1x_3 \\ F_3(x) = -R_{AC,k}i_{d,k} + \omega L_{AC,k}i_{q,k} + \beta c\phi_{dc,k}x_2x_4 - v_{dB} \\ F_4(x) = -\omega L_{AC,k}i_{d,k} - R_{AC,k}i_{q,k} + \beta s\phi_{dc,k}x_2x_4 - v_{qB} \\ F(x) = [F_1\ \ F_2\ \ F_3\ \ F_4]^T. \end{array} \quad (22)$$

The matlab optimization function `fsolve` can be called to determine $F(x)$ every feedforward time step τ_{ff} update or

$$x = fsolve(F(x), x_0)$$

where x_0 is the initial condition for each microgrid k and is used iteratively as the starting condition for each new update. For our specific implementation the OPTI toolbox `opti_fsolve` function was employed [20].

B. Feedback Control

The feedback control design begins with the definition of the error states. The AC/DC microgrid system error state and control inputs are defined as $\tilde{\mathbf{x}} = \mathbf{x}_R - \mathbf{x} = \mathbf{e}$ and $\tilde{\mathbf{u}} = \mathbf{u}_R - \mathbf{u} = \Delta\mathbf{u}$. The feedback control is selected as a PI control

$$\Delta\mathbf{u} = -\mathbf{K_P}\mathbf{B}\tilde{\mathbf{x}} - \mathbf{K_I}\mathbf{B}\int_0^t \tilde{\mathbf{x}}d\tau \tag{23}$$

where $\mathbf{K_P}$ and $\mathbf{K_I}$ are positive definite controller gains. The energy surface or Hamiltonian for the system is determined as the sum of kinetic and potential energies or

$$\mathcal{H} = \frac{1}{2}\tilde{\mathbf{x}}^T\mathbf{M}\tilde{\mathbf{x}} + \frac{1}{2}\left[\int_0^t \tilde{\mathbf{x}}d\tau\right]^T \mathbf{B}^T\mathbf{K_I}\mathbf{B}\left[\int_0^t \tilde{\mathbf{x}}d\tau\right] \quad \forall\tilde{\mathbf{x}} \neq \mathbf{0} \tag{24}$$

which is a positive definite function and defines the AC microgrid static stability condition. The integral controller gain, $\mathbf{K_I}$, provides additional control potential energy to further shape or design the energy surface to meet the static stability condition. The transient performance is determined from the power flow or Hamiltonian rate

$$\dot{\mathcal{H}} = \tilde{\mathbf{x}}^T\left[\mathbf{M}(\dot{\mathbf{x}}_R - \dot{\mathbf{x}})\right] + \tilde{\mathbf{x}}^T\mathbf{B}^T\mathbf{K_I}\mathbf{B}\left[\int_0^t \tilde{\mathbf{x}}d\tau\right]. \tag{25}$$

Substituting for both the reference $\dot{\mathbf{x}}_R$ and $\dot{\mathbf{x}}$ from Eqns (16), (13), and simplifying terms yields the dynamic stability condition

$$-\tilde{\mathbf{x}}^T\left[\mathbf{B}^T\mathbf{K_P}\mathbf{B} - \bar{\mathbf{R}}\right]\tilde{\mathbf{x}} < 0 \quad \forall\tilde{\mathbf{x}} \neq \mathbf{0}. \tag{26}$$

Selection of the proportional controller gain, $\mathbf{K_P}$, determines the transient performance for the AC/DC microgrid system along the Hamiltonian energy surface.

IV. Numerical Simulations

The AC/DC microgrid system model and control was tested and verified with a renewable energy scenario. This scenario included both feedforward/feedback with varying load and one varying generator input. The AC/DC microgrid networked model and control analysis was performed in the Matlab/Simulink environment. (

The HSSPFC controller design from the previous section for both feedback and feedforward control is applied to the AC/DC microgrid networked model shown in Appendix A Fig. 4 and investigated through numerical simulations. Now both the input generation (representative of one varying PV input and two constant diesel generators) are tested along with a varing load profile. These profiles are shown in Fig. 5 for the generator voltage input sources and for the varying load profile shown in Fig. 6. The feedforward solution was updated as a function of the varying input source and load profiles (where $\tau_{ff} = 0.05$ sec). The DC current into the inverter with and without feedback control is shown in Fig. 7. The corresponding DC bus voltage is given in Fig. 8. Typical performance for DC bus voltage regulation is $V_{dc_{nominal}} \pm 5\%$. The D-axis and Q-axis currents along with voltages are shown in Figs. 9-10, respectively. Note there are not any current feedback controllers and these are considered open loop responses (free) for the D-axis and Q-axis currents. The transient performance is improved with the tuned feedback controllers. The DC power levels for each individual microgrid are given in Fig. 13 and are nominally on the order of 30kW tactical microgrid design levels. Note the PV microgrid has a higher variation in power levels. Similar results on the AC power side are shown in Fig. 14 with the sum total for all three microgrids shown on the order of 90kW. The control efforts for all energy storage systems are given in Fig. 15. The related power requirements for each energy storage system are shown in Fig. 16 along with the peak power requirement for energy storage device on DC microgrid one is shown in Fig. 17 which occurs at $t = 0.4$ seconds with a magnitude of 37.5 kW. The corresponding energy storage requirements are shown in Fig. 18. These profiles can be used to size the actual enegy storage devices required to maintain the indicated microgrid perrformance shown in the other simulation results. The other reference states are shown for the DC boost converter side; duty cycles, $\lambda_{s,k}$, given in Fig. 19, the AC boost convert side; duty cycles, $\lambda_{dc,k}$, given in Fig. 20, and the corresponding phase angles, $\phi_{dc,k}$, given in Fig. 21, respectively. All these reference states were used as set points to the feedback controllers or as updates to the model as part of the $\tilde{\mathbf{R}}$ skew-symmetric matrix.

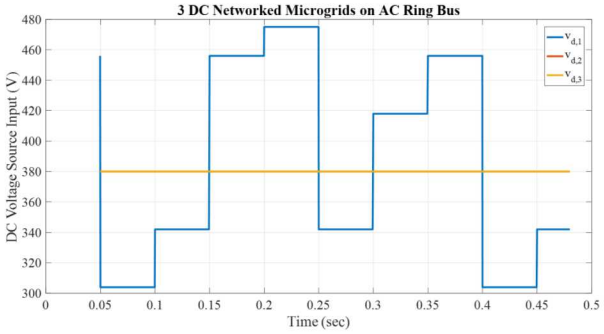

Fig. 5. Variable generator input for microgird 1 and constant generator input for microgrids 2 and 3.

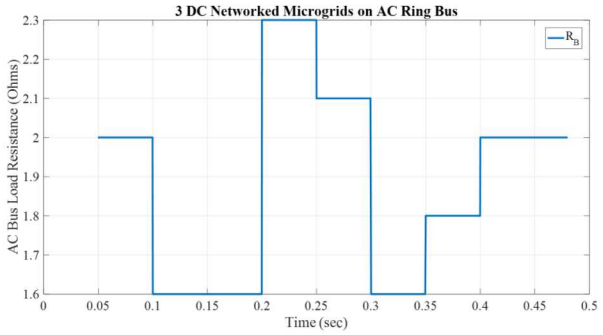

Fig. 6. Variable resistive load on AC ring bus.

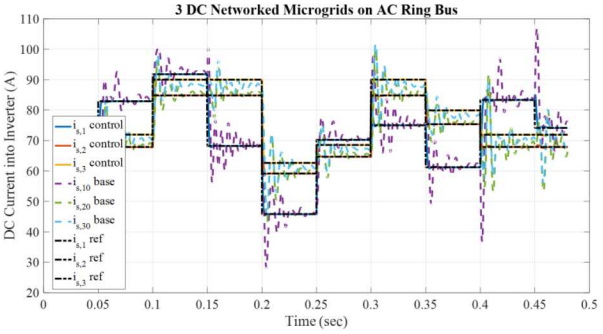

Fig. 7. DC current into inverter with and without controls for microgrid k.

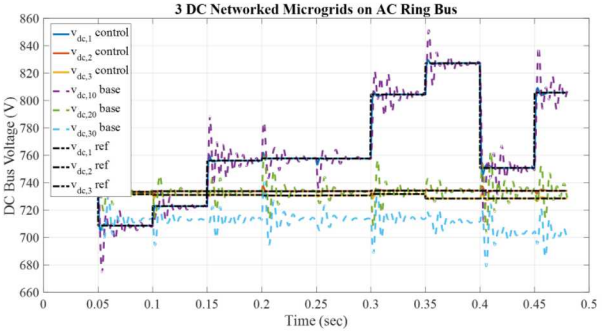

Fig. 8. DC bus voltages with and without controls for microgrid k.

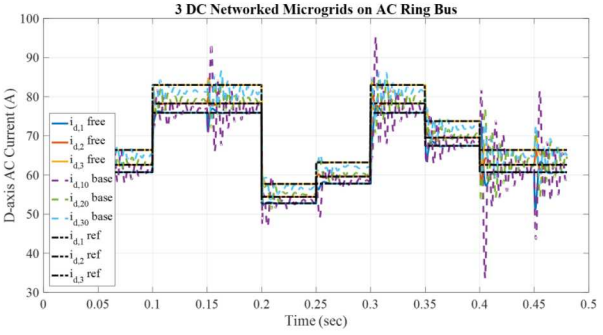

Fig. 9. D-axis current with and without controls for microgrid k.

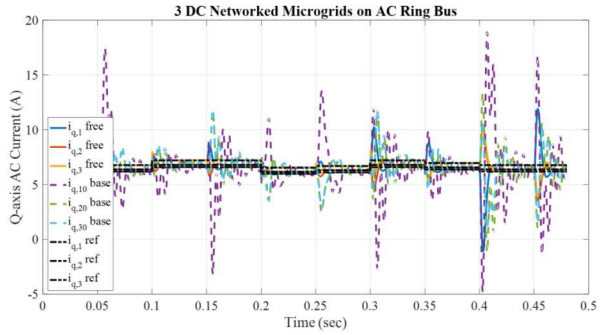

Fig. 10. Q-axis current with and without controls for microgrid k.

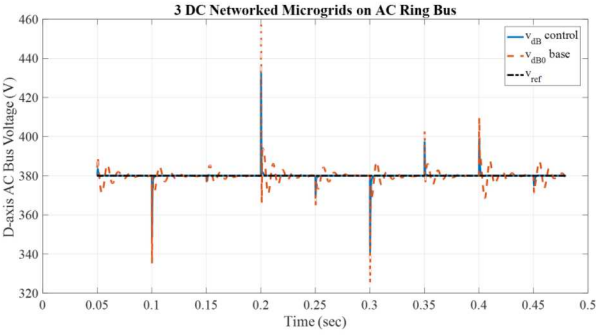

Fig. 11. D-axis bus voltage with and without controls for AC ring bus.

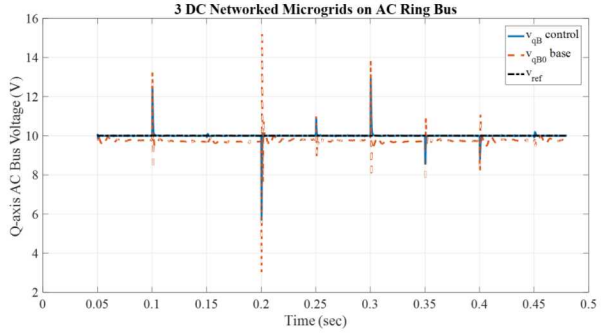

Fig. 12. Q-axis with and without controls for AC ring bus.

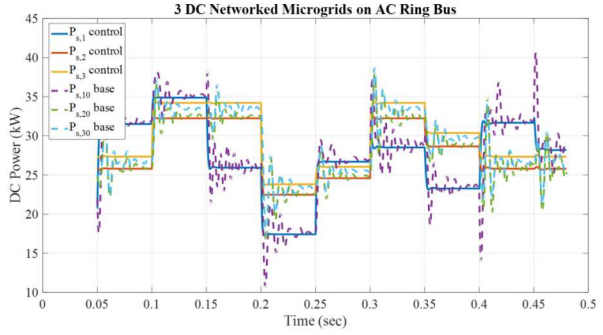

Fig. 13. DC power with and without controls for microgrid k.

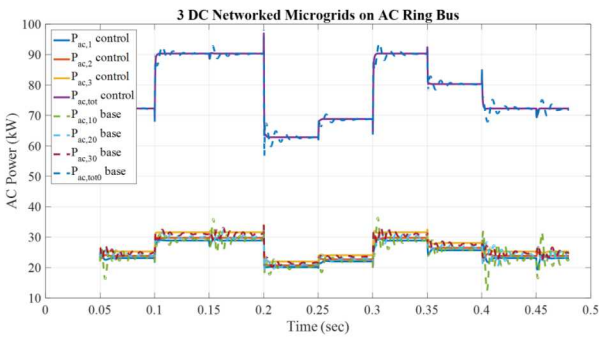

Fig. 14. AC power with and without controls for microgrid k.

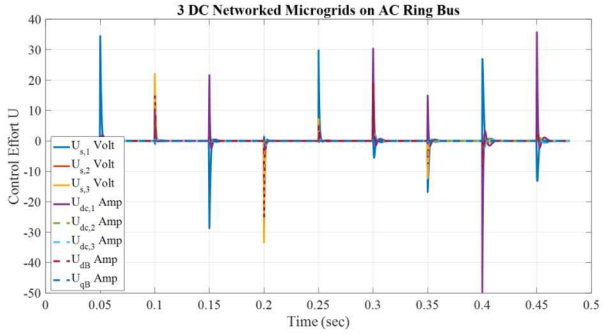

Fig. 15. Control effort for microgrid k.

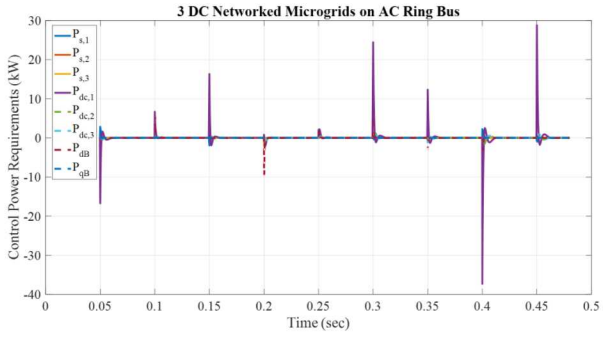

Fig. 16. Control power requirements.

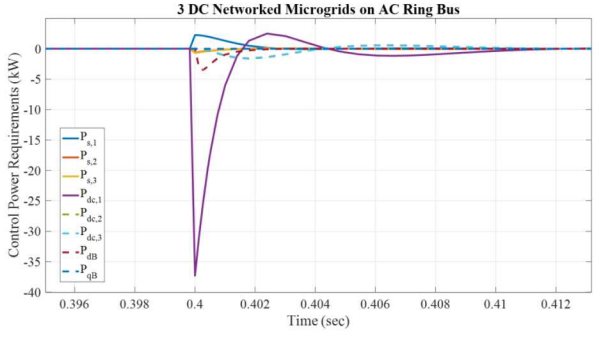

Fig. 17. Control peak power requirement at 0.40 seconds.

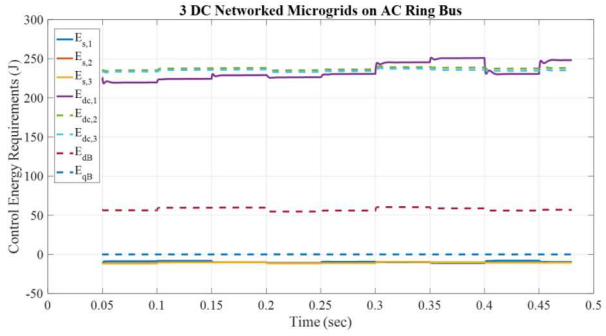

Fig. 18. Control energy requirements.

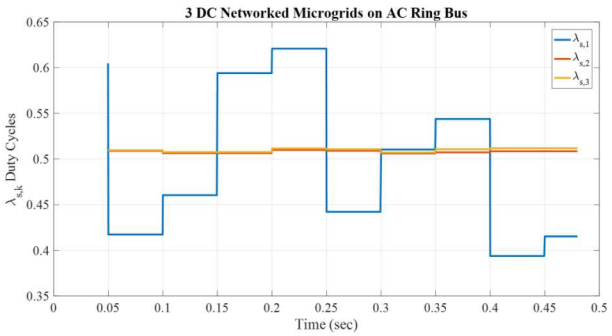

Fig. 19. DC boost converter duty cycles for microgrid k.

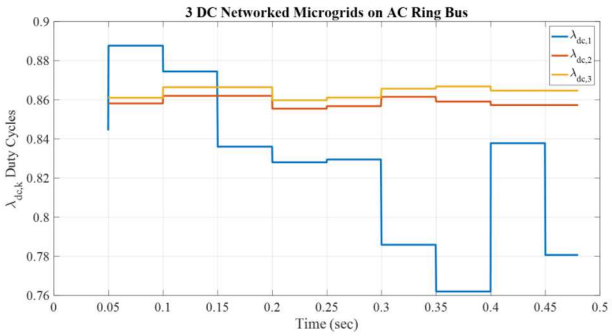

Fig. 20. AC boost inverter duty cycles for microgrid k.

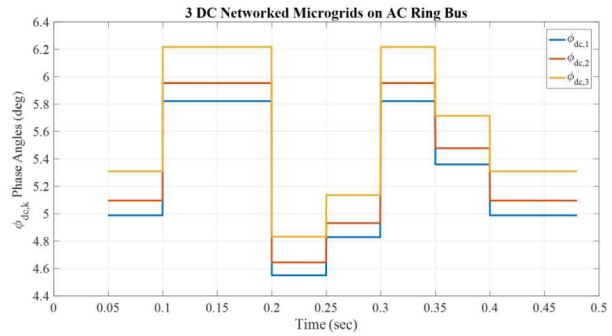

Fig. 21. AC boost inverter phase angles for microgrid k.

V. Summary and Conclusions

In this paper a method for designing feedforward and feedback controllers for integration of stochastic sources and loads into an AC/DC networked microgrid system was presented. A reduced order model was developed for general AC/DC microgrid networked systems that are suitable for HSSPFC control design. A simple feedforward steady state solution was utilized for the feedforward controls block. Feedback control laws were designed for the energy storage systems. A HSSPFC controller design was implemented that incorporated energy storage systems that provided static and dynamic stability conditions for both the DC random stochastic input side and the AC random stochastic load side. Transient performance was investigated for both feedback and feedforward/feedback control, respectively. Numerical simulations were performed and provided power and energy storage profile requirements for the AC/DC microgrid networked system overall performance. The HSSPFC design was impelmented in the Matlab/Simulink environment that is compatible for evaluation on a real-time simulation/controller platform.

Acknowledgments

Sandia National Laboratories is a multimission laboratory managed and operated by National Technology and Engineering Solutions of Sandia, LLC., a wholly owned subsidiary of Honeywell International, Inc., for the U.S. Department of Energy's National Nuclear Security Administration under contract DE-NA0003525. Earlier pioneering research in separate DC and AC microgrid modeling and control investigations was sponsored by a Sandia Grand Challenge Laboratory Directed Research and Development project [21].

References

[1] Robinett R.D. III and Wilson, D.G., **Nonlinear Power Flow Control Design: Utilizing Exergy, Entropy, Static and Dynamic Stability, and Lyapunov Analysis**, Springer-Verlag, London Ltd., Oct. 2011.

[2] Baghaee, H.R., Mirsalim, M., Gharehpetian, G.B., Talebi, H.A., *Decentralized Power Management and Sliding Mode Control Strategy for Hybrid AC/DC Microgrids including Renewable Energy Sources*, IEEE Trans. on Industrial Informatics, 2017 in press, pp. 1-17, Feb. 2017.

[3] Unamuno, E. and Barrera, J.A., *Hybrid AC/DC microgrids - Part II: Review and Classification of Control Strategies*, Renewable and Sustainable Energy Reviews, Vol. 52, Dec 2015, pgs. 1123-1134.

[4] Guerrero, J.M., Loh, P.C., Lee, T.-Z., Chandorkar, M., *Architectures for Intelligent Microgrids - Part II: Power Quality, Energy Storage, and AC/DC Microgrids*, IEEE Trans. on Industrial Electronics, Vol. 60, Issue 4, April 2013.

[5] Kahrobaeian, A. and Mohamed, Y. a.-R. I., *Networked-Based Hybrid Distributed Power Sharing Control for Islanded Microgrid Systems*, IEEE Trans. on Power Electronics, Vol. 30, Issue 2, Feb. 2015.

[6] Guerrero, J.M., Chandorkar, M., Lee, T.-L., Loh, P.C., *Advanced Control Architectures for Intelligent MIcroGrids - Part I: Deventralized and Hierarchical Scheme in Multi-DER Microgrids,* IEEE Trans. Industrial Applications, Vol. 60, No. 4, pp. 1254-1262, April 2013.

[7] Weaver, W.W., Robinett III, R.D., Parker, G.G., and Wilson, D.G., *Distributed Control and Energy Storage Requirements of Networked DC Microgrids*, Control Engineering Practice, Vol. 44, pp. 10-19, 2015.

[8] Luo, F., Lai, Y., Loo, K., Tse, C.K., Ruan, X., *A Generalized Droop-Control Scheme for Decentralized Control of Inverter-Interfaced Microgrids*, in IEEE International Symposium on Circuits and Systems, 2013, pp. 1320-1323.

[9] Weaver, W.W., Robinett III, R.D., Parker, G.G., and Wilson, D.G., *Energy Storage Requirements of DC Microgrids with High Penetration Renewables Under Droop Control*, International Journal of Electrical Power & Energy Systems, Vol. 68, pp. 203-209, 2015.

[10] Di Somma, M., Yan, B., Bianco, N., Graditi, G., Luh, P.B., Mongibello, L., and Naso, V., *Operation Optimization of a Distributed Energy System Considering Energy Costs and Exergy Efficiency*, Energy Conversion and Management, 103 (2015), pp. 739-751.

[11] Young, J., *Optizelle: An open source software library designed to solve general purpose nonlinear optimization problems,* 2014, www.optimojoe.com, Open source software.

[12] Wilson, D.G., Robinett III, R.D., and Goldsmith, S.Y., *Renewable Energy Microgrid Control with Energy Storage Integration*, International Symposium on Power Electronics, Electrical Drives, Automation and Motion, SPEEDAM, June 20-22, 2012, Sorrento, Italy.

[13] Robinett, R.D. III, Wilson, D.G., Eisler, G.R., Hurtado, J.E., **Applied Dynamic Programming for Optimization of Dynamical Systems**, SIAM, Advances in Design and Control Series, July 2005.

[14] Robinett, R.D. III, and Wilson, D.G. *Nonlinear Power Flow Control Design for Combined Conventional and Variable Generation Systems: Part I - Theory,* 2011 IEEE Multi-Conference on Systems and Control, Sept. 26-30, 2011, Denver, Co., USA, pp. 61-64.

[15] Robinett, R.D. III, and Wilson, D.G. *Transient Stability and Performance Based on Nonlinear Power Flow Control Design of Renewable Energy Systems,* 2011 IEEE Multi-Conference on Systems and Control, Sept. 26-30, 2011, Denver, Co., USA, pp. 881-886.

[16] Hassell, T., Weaver, W.W., Robinett III, R.D., Wilson, D.G., Parker, G.G., *Modeling of Inverter Based AC Microgrids for Control Development*, IEEE MSC Conference, Sydney, Australia, September 20-22, 2015.

[17] Wilson, D.G., Neely, J., Cook, M., Glover, S., Young, J., Robinett III, R.D., *Hamiltonian Conrol Design for DC Microgrids with Stochastic Sources and Loads with Applications*, in IEEE International Symposium on Power Electronics, Electrical Drives, Automation and Motion, SPEEDAM, 2014, pp. 1264-1271.

[18] Wilson, D.G., Robinett III, R.D., Weaver, W.W., Byrne, R.H, Young, J., *Nonlinear Power Flow Control Design of High Penetration Renewable Sources for AC Inverter Based Microgrids*, in IEEE International Symposium on Power Electronics, Electrical Drives, Automation and Motion, SPEEDAM, June 22-24, 2016, AnaCapri, Italy.

[19] Robinett III, R.D., Wilson, D.G., Goldsmith, S.Y., *Customized Electric Power Storage Device for Inclusion in a Collective Microgrid*, US Patent, US 9,263,894, Feb. 16, 2016.

[20] Currie, J., OPTI Toolbox, A Free MATLAB Toolbox for Optimization, invP, December 2016.

[21] Glover, S.F., *et. al.*, *Enabling Secure Scalable Microgrids for High Penetration Renewables: Final Report for LDRD Project #152503*, Sandia National Laboratories, Sand Report SAND2013-10704, December 2013.